

Geometric phases and the Sagnac effect: Foundational aspects and sensing applications

I. L. Paiva, R. Lenny, and E. Cohen

*Faculty of Engineering and the Institute of Nanotechnology and Advanced Materials,
Bar-Ilan University, Ramat Gan 5290002, Israel*

Geometric phase is a key player in many areas of quantum science and technology. In this review article, we outline several foundational aspects of quantum geometric phases and their relations to classical geometric phases. We then discuss how the Aharonov-Bohm and Sagnac effects fit into this context. Moreover, we present a concise overview of technological applications of the latter, with special emphasis on gravitational sensing, like in gyroscopes and gravitational wave detectors.

I. INTRODUCTION

The fundamental notion of geometric phase [1–3] has been highly influential in physics and related sciences. It lies at the heart of many quantum phenomena pertaining to basic science and at the same time delineates important technological applications for quantum sensing and quantum computation.

Various geometric phases were originally introduced as a result of physical systems undergoing adiabatic cyclic evolution. However, this notion was extended with the removal of the adiabatic and even the cyclic conditions. In this work, we intend to review fundamental aspects underlying these phases and present some of their practical applications, such as in gyroscopes and Laser Interferometer Gravitational-Wave Observatory (LIGO) detectors.

Differently from other review articles on the subject, see, e.g., Refs. [4–8], we focus on the relation between geometric phases and accelerating as well as gravitational systems. In particular, we give special emphasis on quantum applications of the Sagnac effect in such systems. At the same time, much more attention is given to geometric phases here than in review articles specialized on Sagnac interferometers, such as Refs. [9–11].

The paper is organized as follows. Section II discusses the geometry underlying quantum systems. From this structure, geometric phases are introduced in Section III. This section also compares quantum geometric phases with classical ones. The Aharonov-Bohm (AB) effect, which is associated with a special — i.e., topological — type of geometric phase, is presented in Section IV. Following that, Section V discusses geometric phases in non-inertial frames and introduces the Sagnac effect. Then, Section VI presents various applications of the Sagnac effect for quantum sensing and metrology. Section VII presents geometric and gravitational AB-like effect and discuss their relevance in the present context. Finally, Section VIII concludes the paper with some future outlook.

II. GEOMETRY OF QUANTUM STATES

In this section, we present the geometry underlying the mathematical structures of quantum states. Although

the formal name of each structure is mentioned, we restrict our presentation to the intuition behind them. For a more technical exposition, we refer the reader to, e.g., Refs. [12, 13].

Consider a pure quantum system represented by a state in a complex Hilbert space $\mathcal{H}_{n+1} \setminus \mathcal{O}$, where $n \in \mathbb{N}$, $n+1$ is the dimension of the space, and \mathcal{O} . Because of the probabilistic interpretation, it is conventional to work with normalized vectors. Also, states that differ only by a global phase are indistinguishable. Then, two non-null vectors $|\psi\rangle$ and $|\varphi\rangle$ in \mathcal{H}_{n+1} represent the same physical state if there exists $\lambda \in \mathbb{C}$ such that

$$|\psi\rangle = \lambda|\varphi\rangle. \quad (1)$$

Then, while $n+1$ complex parameters are needed to characterize a vector in \mathcal{H}_{n+1} , n suffices to characterize a pure quantum state.

Eq. (1) effectively defines an equivalence relation in \mathcal{H}_{n+1} , subdividing the space into *equivalence classes*. In fact, denoting this relation by \sim , we can write

$$|\psi\rangle \sim |\varphi\rangle \quad (2)$$

whenever there exists $\lambda \in \mathbb{C}$ such that Eq. (1) is satisfied. Here, again, $|\psi\rangle$ and $|\varphi\rangle$ are non-null vectors in \mathcal{H}_{n+1} .

The resultant space after the operation \sim is applied to entire $\mathcal{H}_{n+1} \setminus \mathcal{O}$ is the *projective space*, also known as *ray space*,

$$\mathbb{CP}(n) \equiv \frac{\mathcal{H}_{n+1} \setminus \mathcal{O}}{\sim}, \quad (3)$$

which is an n -dimensional complex space.

It is typically convenient to treat \sim as a composition of two distinct equivalence relations. One of them, denoted by \sim_S is such that any two vectors $|\psi\rangle$ and $|\varphi\rangle$ vectors in $\mathcal{H}_{n+1} \setminus \mathcal{O}$ are equivalent, i.e.,

$$|\psi\rangle \sim_S |\varphi\rangle, \quad (4)$$

whenever there exists $\rho \in \mathbb{R}$ such that

$$|\psi\rangle = \rho|\varphi\rangle. \quad (5)$$

It can be checked that the resultant space is isomorphic to the unity $2n+1$ -dimensional real hyper-sphere S_{2n+1} ,

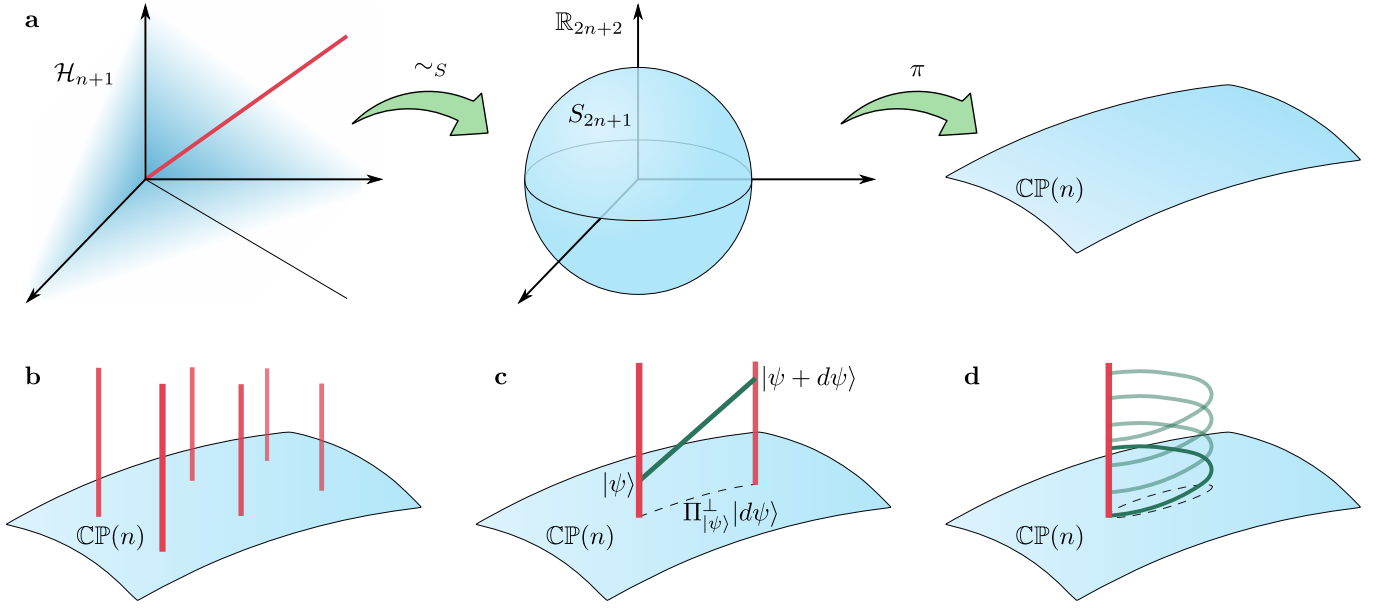


FIG. 1. Geometric representation of pure quantum systems whose state is an element of a complex Hilbert space \mathcal{H}_{n+1} , which is isomorphic to a real vector space of dimension $2n + 2$. **(a)** An arbitrary direction of the Hilbert space, like the red line, represents a single physical state. Then, restricting to normalized vectors with an equivalence relation \sim_S , the resulting space is isomorphic to a real hypersphere S_{2n+1} . Finally, a projector π can map each point that differs by a global phase to a single element of a complex projective space $\mathbb{CP}(n)$. **(b)** The global phases, thus, can be represented by tangent fibers to each point of $\mathbb{CP}(n)$. **(c)** Using the fiber bundle structure, a notion of distance can be naturally introduced in $\mathbb{CP}(n)$ since the projector of orthogonal direction to a certain state $|\psi\rangle$, represented by $\Pi_{|\psi\rangle}^\perp$ is well-defined. **(d)** Moreover, a system that completes a loop in $\mathbb{CP}(n)$ does not always return to its initial point in the bundle structure. This lack of holonomy constitutes the geometric origins of geometric phases.

as represented in Figure 1a. In fact, with the relation \sim_S , the $n + 1$ complex parameters (or $2n + 2$ real ones) necessary to characterize a state in \mathcal{H}_{n+1} are constrained by an equation that establishes the unit norm, which results in $2n + 1$ free real parameters necessary for the characterization of a state. Because of this isomorphism, the space associated with \sim_S will be referred to as the hypersphere S_{2n+1} .

To complete the relation \sim , a map π , also associated with an equivalence relation, is applied to the elements of S_{2n+1} , mapping them into a representative element of their class in $\mathbb{CP}(n)$, as illustrated in Figure 1a. Observe that if two points associated with the normalized vectors $|\psi\rangle$ and $|\varphi\rangle$ are such that

$$\pi(|\psi\rangle) = |\varphi\rangle, \quad (6)$$

then there exists $\theta \in \mathbb{R}$ such that

$$|\psi\rangle = e^{i\theta}|\varphi\rangle, \quad (7)$$

i.e., they differ by a global phase. Hence, these phases can be seen as fibers with circular topology at each point of $\mathbb{CP}(n)$, as represented in Figure 1b. In fact, this constitutes a *fiber bundle* structure, where $\mathbb{CP}(n)$ is the base space, the space of the phases is the fiber, S_{2n+1} is the total space, and π is the projection map, also known as bundle projection.

It can be shown that the space $\mathbb{CP}(n)$ inherits the symplectic structure of \mathcal{H}_{n+1} , i.e., a well-defined notion of hypervolume [13]. Thus, the projection of the temporal evolution of the unitary dynamics on $\mathbb{CP}(n)$ is a Hamiltonian dynamics.

In addition to this structure, $\mathbb{CP}(n)$ also acquires the metric induced by the inner product in \mathcal{H}_{n+1} . It is, then, possible to compute the distance between two points in $\mathbb{CP}(n)$. In fact, let $|\psi\rangle$ and $|\psi+d\psi\rangle$ be infinitesimally close in S_{2n+1} . Then, as illustrated in Figure 1c, a natural definition for the distance in $\mathbb{CP}(n)$ between them is

$$ds^2(\mathbb{CP}(n)) \equiv K \langle d\psi | \Pi_{|\psi\rangle}^\perp | d\psi \rangle, \quad (8)$$

where K is a positive real constant, $\Pi_{|\psi\rangle}^\perp \equiv I - |\psi\rangle\langle\psi|$ is the projector in the orthogonal direction to $|\psi\rangle$, and $|d\psi\rangle = |\psi+d\psi\rangle - |\psi\rangle$. Interestingly, if $|\psi+d\psi\rangle$ is such that $|\psi+d\psi\rangle = |\psi(t+dt)\rangle$, i.e., is the result of an evolution in time generated by a Hamiltonian H , we obtain

$$|d\psi(t)\rangle = |\psi(t+dt)\rangle - |\psi(t)\rangle = -\frac{i}{\hbar} H |\psi(t)\rangle dt \quad (9)$$

from the Schrödinger equation. Then, the distance be-

tween these two states in $\mathbb{CP}(n)$ is

$$\begin{aligned} ds^2(\mathbb{CP}(n)) &= K(\langle d\psi|d\psi\rangle - \langle d\psi|\psi\rangle\langle\psi|d\psi\rangle) \\ &= \frac{K}{\hbar^2}(\langle\psi|H^2|\psi\rangle - \langle\psi|H|\psi\rangle^2) dt^2 \\ &= \frac{K}{\hbar^2}(\Delta H)^2 dt^2, \end{aligned} \quad (10)$$

i.e., the “velocity” of the system in $\mathbb{CP}(n)$ is proportional to the uncertainty of its energy, as shown by Anandan and Aharonov [14].

Interestingly, it follows from the Schrödinger equation that the distance between two states $|\psi(t)\rangle$ and $|\varphi(t)\rangle$ evolving under the same Hamiltonian do not change in time since

$$\frac{d}{dt}(\langle\psi(t)|\varphi(t)\rangle) = 0 \quad (11)$$

and Eq. (8) implies that, in $\mathbb{CP}(n)$, the distance $s(|\psi\rangle, |\varphi\rangle)$ between two states $|\psi\rangle$ and $|\varphi\rangle$ is such that

$$s^2(|\psi\rangle, |\varphi\rangle) = K(1 - |\langle\psi|\varphi\rangle|^2). \quad (12)$$

Physically, this means that the probability of transition between these two states is also preserved. In particular, if $|\psi(t)\rangle = |\varphi(t)\rangle$, it follows that the norm of vectors is kept constant in time. In other words, the evolution of a state creates a trajectory in S_{2n+1} , which can, then, be projected into $\mathbb{CP}(n)$.

Another important aspect is that, although the global phase of a state vector has no physical meaning, the phase difference between two states has. It is even possible to define a *connection* in S_{2n+1} by establishing that, given two states $|\psi\rangle$ and $|\psi+d\psi\rangle$ projected into points infinitesimally close to each other in $\mathbb{CP}(n)$, they are parallel to each other in S_{2n+1} if the phase difference between them is null, i.e.,

$$\arg(\langle\psi|\psi+d\psi\rangle) = 0. \quad (13)$$

With the connection, the concept of *parallel transport* can be introduced. Given a curve in $\mathbb{CP}(n)$ represents an infinite number of curves in S_{2n+1} . A subset of special interest is the one for which the curves are defined on geodesics in S_{2n+1} , i.e., the curves built through parallel transport in S_{2n+1} . These trajectories are characterized by

$$\langle\psi(s)|\frac{d}{ds}|\psi(s)\rangle = 0 \quad (14)$$

along the curve defined by $|\psi(s)\rangle$ in terms of a real parameter s . Each of these curves is called a *geodesic lifting* of the curve in $\mathbb{CP}(n)$. A geodesic lifting does not have intrinsic physical meaning — only the family of geodesic liftings has. This is illustrated in Figure 1d, where all geodesic liftings (green curves) have an equivalent physical meaning.

Besides its significance to the study of geometric phases, as it will be discussed in the next section, the

geometric structure presented here was used for a pedagogical approach to the quantum adiabatic theorem [15] and signaling in Weinberg’s non-linear quantum mechanics [16]. Also, this structure provides a geometric interpretation to von Neumann’s measurement interaction model, weak values, and quantum erasers [17, 18], and can be used for the introduction of a type of time-energy uncertainty relation [14]. Finally, this structure is also the same that appears in Yang-Mills theories, which underlie the standard model of particle physics.

III. GEOMETRIC PHASES

As a consequence of the geometry discussed in the previous section, when a system completes a closed cycle in $\mathbb{CP}(n)$, its trajectory is not necessarily closed in S_{2n+1} . A measure of this lack of *holonomy* can be locally defined at each point of $\mathbb{CP}(n)$ by considering an infinitesimal closed curve around each point. This quantity corresponds to the *curvature* of the connection and is the mathematical structure in which we are interested. In fact, this structure stands behind the geometric (or non-integrable) phase, as represented in Figure 1d.

To see that, assume a system, initially in the state $|\psi(0)\rangle$, completes a cyclic evolution of period τ in $\mathbb{CP}(n)$. Then, we can write its final state as

$$|\psi(\tau)\rangle = e^{i\phi}|\psi(0)\rangle. \quad (15)$$

Part of the phase it acquires is the dynamical phase

$$\phi_{\text{dyn}}(\tau) = -\frac{1}{\hbar} \int_0^\tau \langle\psi(t)|H(t)|\psi(t)\rangle dt, \quad (16)$$

where $H(t)$ is the Hamiltonian that governs the dynamics of the system. However, Berry noted that, in the adiabatic regime, the system in fact accumulates an extra phase, which became known as the *Berry phase* [1]. This extra phase is geometric and corresponds to the lack of holonomy we just discussed, as it was shown by Simon [19]. Because of it, the natural connection introduced above is known as the Berry-Simon connection. Later on, the adiabatic condition was removed by Aharonov and Anandan [20]. In fact, defining

$$|\tilde{\psi}(t)\rangle \equiv e^{-i[f(t)+\phi_{\text{dyn}}(t)]}|\psi(t)\rangle, \quad (17)$$

where f is a function such that $\phi - \phi_{\text{dyn}}(\tau) = f(\tau) - f(0)$, it follows that $|\tilde{\psi}(\tau)\rangle = |\tilde{\psi}(0)\rangle$ and

$$i\hbar \frac{d}{dt}|\tilde{\psi}(t)\rangle = \left[H(t) + \hbar \frac{d}{dt}f(t) - \langle\psi(t)|H(t)|\psi(t)\rangle \right] |\tilde{\psi}(t)\rangle, \quad (18)$$

which, in turn, implies that

$$\frac{d}{dt}f(t) = \langle\tilde{\psi}(t)|\left(i\frac{d}{dt}\right)|\tilde{\psi}(t)\rangle, \quad (19)$$

regardless of H . Then, after ending the cycle, the state $|\psi\rangle$ accumulates an extra phase $\phi_{\text{geom}} \equiv f(\tau) - f(0)$ that can be expressed as

$$\phi_{\text{geom}} = \int_0^\tau \langle \tilde{\psi}(t) | \left(i \frac{d}{dt} \right) | \tilde{\psi}(t) \rangle dt = i \oint_C \langle \tilde{\psi}(R) | d\tilde{\psi}(R) \rangle, \quad (20)$$

which can be shown to depend only on geometric properties associated with the cycle, thus, in particular, is not a function of τ . The last integral in Eq. (20) is taken over a curve C in the parameter space, which has a parameter R associated with it. These phases are present and play a fundamental role in the properties of many physical systems in nature, like in molecular systems [21] and crystalline dielectrics [22].

Geometric phases can be introduced for mixed states [23, 24]. In fact, they are studied in open and non-Hermitian systems [25–33]. However, an important remark that should be presented here is that, depending on how it is extended to the dynamics of non-Hermitian Hamiltonians, the phase introduced by Aharonov and Anandan always assumes real values. In this case, the adiabatic limit of ϕ_{geom} does not always correspond to the Berry phase [34]. Moreover, in general scenarios, these phases can be studied in systems with non-cyclic evolution and even when intermediate measurements are taken into account [35].

Also, geometric phases can be introduced for classical systems undergoing adiabatic evolution, as it was shown by Hannay [36]. In fact, for integrable systems, one can represent the Hamiltonian that governs the evolution in terms of action-angle coordinates [37]. It can be, then, concluded that the evolution is defined in a torus in phase space. In cyclic adiabatic evolutions, action coordinates are preserved while angle coordinates may change. Hannay observed that these changes in angle coordinates during a cycle have dynamical and geometrical contributions, in a similar manner first observed by Berry for quantum systems. The geometrical contribution is what became known as the Hannay angle. From a more geometrical perspective, the Cartesian product between the parameter space and the phase-space defined a trivial fiber over the parameter space. Within this structure, the Hannay angle is, then, obtained from liftings in the total space according to a connection known as the Hannay-Berry connection [12, 13, 38]. Then, like for Berry phases, the notion of a Hannay angle for open paths can also be considered [39].

It should be noted that the notion of geometric phases can be extended to classical dissipative systems [40]. Moreover, perturbative methods can be used for non-adiabatic correction in some scenarios [41]. However, the corrections are not purely geometric since, in general, they depend on the time-parametrization of the trajectories. Furthermore, geometric phases are also studied in nonlinear classical field theories [42–44].

Given a Hamiltonian of an integrable system and denoting the action variable by $I = \{I_0, \dots, I_{n-1}\}$, it is possible to find a direct mathematical relation between

the Hannay angle $h(I; C)$ and the Berry phase $\phi(C)$ acquired by a physical system during a cyclic evolution through a path C . This follows from the use of the Bohr-Sommerfeld quantization rule, in which each I_j is quantized as $I_j = \hbar(n_j + \mu_j/4)$, where μ_j is a *Maslov index*, which is a topological quantity, and n_j is an integer. This, combined with further analysis of the geometrical structure permeating both phases, leads to [13, 45]

$$\frac{\partial \phi(C)}{\partial n_j} = -h(I; C) + O(\hbar). \quad (21)$$

While this implies that the Hannay angle may vanish in scenarios where the Berry phase differs from zero, the converse does not hold: the Berry phase cannot vanish if the Hannay angle is null.

This type of relation makes the ability to discriminate quantum and classical contributions to interference experiments an important issue, which was already considered, e.g., in optomechanical systems [46]. Also, it can be argued that geometric phases observed in various experiments with light-waves — not matter-waves — are Hannay angles [47]. This is the case because the Berry phase becomes proportional to the Hannay angle. In this regard, the use of squeezing Hamiltonians was suggested as a possible way to make Berry phases detectable in these experimental setups [48–50].

Before concluding this section, we call attention to the fact that, in cases of Hamiltonians with degeneracy, geometric phases (both quantum and classical) become non-Abelian [51, 52].

IV. AHARONOV-BOHM EFFECT

An important type of geometric phase is the phase associated with the AB effect. In classical physics, the dynamics of a particle with charge q is only affected by a magnetic field that directly interacts with it, i.e., if the particle travels in a region where the magnetic field is non-zero. However, in quantum mechanics, this is not always the case. In fact, suppose a charge encircles a region in space that contains a magnetic field. Then, it accumulates a quantum phase proportional to the magnetic flux inside the region enclosed by its trajectory, regardless of whether there was any magnetic field on the particle's trajectory.

In 1939, this effect might have been hinted at by Franz in a talk at a physical society meeting in Danzig [53]. Later, in 1949, the effect was presented by Ehrenberg and Siday [54], although the influence of magnetic field in the particle's dynamics seemed to be a peculiar feature of the optical configuration considered by them. The authors themselves wrote: “One might therefore expect wave-optical phenomena to arise which are due to the presence of a magnetic field but not due to the magnetic field itself, i.e., which arise whilst the rays are in field-free regions of space.” It was only in 1959 that the fundamental nature of the effect was revealed in a seminal article by Aharonov

and Bohm [55], the reason for which it is known as the AB effect. More details on early historical aspects of the discovery of the effect can be found in Ref. [56]. Since Aharonov and Bohm's work, the AB effect has been vastly investigated in theoretical and experimental works [57–87].

This effect is usually presented by considering a charge encircling a solenoid whose axis lies, say, on the z axis. For simplicity, the solenoid is taken to be infinitely thin and is sometimes referred to as a *flux line*. Also, for simplicity, the particle is assumed to travel in the xy plane, having the superposition state

$$|\Psi\rangle = \frac{1}{\sqrt{2}}(|\psi_L\rangle + |\psi_R\rangle), \quad (22)$$

where $|\psi_L\rangle$ is a wavepacket that passes to the left and $|\psi_R\rangle$ is a wavepacket that passes to the right of the flux line. This superposition can be achieved, for instance, with the use of a double-slit or a beamsplitter. The Hamiltonian of the particle, in this case, can be written as

$$H = \frac{1}{2m} [\vec{P} - q\vec{A}(\vec{Q})]^2, \quad (23)$$

where $\vec{P} = P_x\hat{x} + P_y\hat{y}$, $\vec{Q} = X\hat{x} + Y\hat{y}$, and \vec{A} is the vector potential associated with the solenoid, which can take different forms according to the choice of gauge.

To obtain the solution of this Hamiltonian, let the states $|\psi_L^0\rangle$ and $|\psi_R^0\rangle$ be the solutions in the case where there is no magnetic field, i.e., $H_0 = P^2/2m$. Then, based on a procedure introduced by Dirac [88], it can be obtained that, after the left and the right wavepackets travel, respectively, the trajectories γ_L and γ_R ,

$$|\psi_L\rangle = e^{iq \int_{\gamma_L} \vec{A} \cdot d\vec{\ell}/\hbar} |\psi_L^0\rangle \quad (24)$$

and

$$|\psi_R\rangle = e^{iq \int_{\gamma_R} \vec{A} \cdot d\vec{\ell}/\hbar} |\psi_R^0\rangle. \quad (25)$$

Now, recall that quantum states are equivalent up to a global phase and observe that

$$\int_{\gamma_R} \vec{A} \cdot d\vec{\ell} - \int_{\gamma_L} \vec{A} \cdot d\vec{\ell} = \oint \vec{A} \cdot d\vec{\ell}, \quad (26)$$

which is independent of the path $\gamma_R - \gamma_L$ and has physical significance since it corresponds to the magnetic flux Φ_B inside the region enclosed by the charge. Then, the state of the system after it encircles the flux line is

$$|\Psi\rangle = \frac{1}{\sqrt{2}}(|\psi_L^0\rangle + e^{i\Delta\phi_{AB}}|\psi_R^0\rangle), \quad (27)$$

where

$$\Delta\phi_{AB} \equiv \frac{q}{\hbar} \oint \vec{A} \cdot d\vec{\ell} \quad (28)$$

is the quantum phase accumulated by the charge, usually called the AB phase.

To verify that the AB phase is indeed a geometric phase, observe that, for a wavepacket Ψ with center at $\vec{\ell}$ encircling the solenoid, the inner product $\langle\Psi(\vec{r} - \vec{\ell})|\vec{\nabla}_{\vec{\ell}}\Psi(\vec{r} - \vec{\ell})\rangle$ results in

$$\int \Psi^*(\vec{r} - \vec{\ell}) \left[-i\frac{q}{\hbar}\vec{A}(\vec{\ell}) + \vec{\nabla}_{\vec{\ell}} \right] \Psi(\vec{r} - \vec{\ell}) d^3r = -i\frac{q}{\hbar}\vec{A}(\vec{\ell}). \quad (29)$$

Then, replacing it in Eq. (20),

$$\phi_{\text{geom}} = i \oint_C \langle\Psi|\vec{\nabla}_{\vec{\ell}}\Psi\rangle \cdot d\vec{\ell} = \Delta\phi_{AB}. \quad (30)$$

Differently from various geometric phases, however, the AB phase does not depend on the path which \vec{A} is integrated over, as already mentioned, which is one of the reasons it can be considered a *topological phase*. Also, because there always exists a gauge in which vector potential vanishes in an arbitrary region that does not completely enclose the solenoid, *a priori*, the AB effect cannot be seen as the result of the local interaction between the charge and the vector potential. As a result, it is typically considered to be of nonlocal nature. However, there is no final consensus on this issue and, thus, the origins of this phase are investigated until this day with works that include the idea of modular variables [60] and models that consider the source of magnetic field as part of the dynamics or quantize the magnetic field itself [84, 89–101]. Furthermore, the interplay between Berry and AB phases in various scenarios can also be of interest. For instance, the phases acquired by a quantum charge with a large spreading while it encircles one or multiple solenoids were studied in Ref. [102].

To conclude this section, we note that an electric AB effect was also proposed in the seminal article by Aharonov and Bohm [55]. Moreover, a similar effect to the (magnetic) AB effect for neutral particles with a magnetic moment was later proposed by Aharonov and Casher [103]. This effect, often referred to as the Aharonov-Casher effect, was further studied and experimentally verified in various scenarios [104–107].

V. GEOMETRIC PHASES AND NON-INERTIAL EFFECTS

In 1913, Sagnac showed that angular rotation could be detected using interferometers in a classical setup [108]. The configuration introduced by him is now known as the Sagnac interferometer. His result had been anticipated in two publications by Lodge [109, 110], a prediction that, in turn, can be traced back to unpublished correspondences between Lodge and Larmor [10]. This interferometer typically consists of two light beams enclosing a certain region with area a , which is rotating with angular speed ω , as represented in Figure 2. Because of the rotation of the region, the interference of the wavepackets

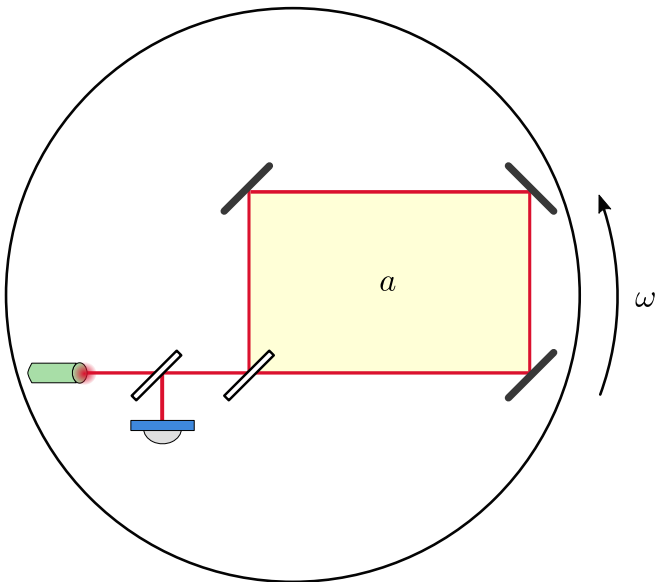


FIG. 2. **Schematic representation of a standard Sagnac interferometer.** Two beams or wavepackets travel an interferometer in opposite directions. If the interferometer is rotating with angular speed ω , the interference pattern is shifted by an amount that depends on ω and the area a enclosed by the interferometer.

is shifted by a phase

$$\Delta\phi_S = \frac{8\pi a\omega}{c\lambda}, \quad (31)$$

where λ is the initial wavelength of the photon. Based on this idea, in 1925, Michelson, Gale, and Pearson conducted an experiment to measure the effects of Earth's rotation on the speed of light [111].

One could, then, wonder whether such an effect had a quantum analog. This is indeed the case, as it was experimentally verified, for instance, by Collela, Overhauser, and Werner [112], based on a previous theoretical proposal [113], and by Werner, Staudenmann, and Colella [114]. Nevertheless, it is possible to make distinctions between the “classical” and “quantum” Sagnac effects [115–117]. In particular, in the nonrelativistic regime, there is no classical Sagnac effect, while the quantum version of it exists. However, in the relativistic limit, they become equivalent. Also, in the relativistic case, rotations of the interferometer or any other non-inertial influences are not required for the existence of a phase difference between the beams or wavepackets. In fact, because of the Doppler shift, the Sagnac effect can be obtained from a loop in space and relative motion — even if both of the systems of reference involved are inertial [118].

The Sagnac effect is, of course, not exclusive to light-waves. In fact, it was observed in neutrons [112], electrons [119], and atoms [120]. One may even consider a Sagnac effect for the superfluid Josephson interferometer [121]. This varied of systems is particularly relevant be-

cause, for precision purposes, we may benefit from the use of matter-waves since they have lower wavelengths, which increases the Sagnac phase-shift and the resulting sensitivity of the interferometer [122]. An analogous way to see this is by observing that the ratio between the rest mass m of a particle and the effective mass $\hbar\omega/c^2$ of a light-wave with frequency ω amounts to a value with eleven orders of magnitude if the particle is an atom and the light-wave is an optical photon in the visible regime [120, 123]. Then, if the Sagnac effect is seen as the result of the rotation of the interfering systems, matter-wave systems highly outperform light-wave systems in interferometers with equal areas. At the same time, optical systems have the advantage of higher particle fluxes and, typically, larger enclosed areas. Still, generally speaking, matter-wave systems are expected to outperform optical systems by several orders of magnitude [120].

To see how the Sagnac effect is manifest for massive particles, we start from a classical analysis of a particle in a rotating system. Such a particle is subject to a Coriolis force given by

$$\vec{F} = 2m\vec{u} \times \vec{\omega}, \quad (32)$$

where \vec{u} indicates the velocity of the system (in the rotating system). Considering the potential vector $\vec{A}_r = \vec{\omega} \times \vec{r}$, we can write $\vec{w} = \vec{\nabla} \times \vec{A}_r$ and

$$\vec{F} = 2m\vec{u} \times (\vec{\nabla} \times \vec{A}_r). \quad (33)$$

From that, a Lagrangian can be defined, followed by its associated Hamiltonian

$$H = \frac{1}{2m} \left(\vec{P} - 2m\vec{A}_r \right)^2 = \frac{1}{2m} \left(\vec{P} - \frac{4\pi\hbar}{c\lambda} \vec{A}_r \right)^2. \quad (34)$$

This Hamiltonian, in turn, can be quantized. In this case, it implies that, according to the direction of motion, a wavepacket acquires a phase of $\pm 4\pi a\omega/c\lambda$. Then, a system in a superposition of wavepackets moving in opposite directions ends up with a relative phase given by Eq. (31).

A more direct way to see this type of influence of non-inertial frames on the dynamics of quantum systems follows the reasoning presented in Ref. [124]. There, the authors showed that the dynamics of a free particle, i.e., a particle whose Hamiltonian is $H = (P_x^2 + P_y^2)/2m$ in a rotating frame is described by a Hamiltonian with a term that is similar to a vector potential. In fact, if ω is the angular speed of the frame about the z axis, the Hamiltonian H' of the particle from the perspective of the rotating frame is a transformation of H by the unitary $\exp(-iL_z\omega/\hbar)$, which in first order becomes

$$H' \approx \frac{1}{2m} \left[(P_x + m\omega Y)^2 + (P_y - m\omega X)^2 \right] \quad (35)$$

if the particle has an orbit with a well-defined radius. From Eqs. (40) and (35), we see that the rotation takes the usual place of the vector potential in the Hamiltonian.

From this discussion, we should expect a relation between the interference in the Sagnac interferometer and the AB effect. This is, in fact, the case, and it was presented in [125]. Before discussing this result, we point out several differences between the two effects, e.g. while the AB effect is given in terms of \hbar and vanishes in the classical limit, this is not the case for the Sagnac effect. In addition, the AB effect is topological while this effect is geometric.

By considering the setup with a rotating single mode optical fiber loop, the authors of Ref. [125] first observed that the relative phase accumulated by each wavepacket is given by

$$\Delta\phi_S = \frac{4\pi\vec{v} \cdot \Delta\vec{\ell}}{c\lambda}, \quad (36)$$

where \vec{v} is the velocity of the fiber and $\Delta\ell$ is the length of a segment of the optical fiber. However, the important novelty of their work is that they also considered a more general scenario where only a portion of the circuit was moving. With that, they were able to gather evidence for the (expected) validity of the general expression for the phase $\Delta\phi_S$, which is

$$\Delta\phi_S = \frac{4\pi}{c\lambda} \oint_{\ell} \vec{v} \cdot d\vec{\ell}. \quad (37)$$

Comparing with the AB phase in Eq. (28), it can be seen that the parallel works with the mapping

$$\vec{A} \rightarrow \frac{4\pi\hbar}{qc\lambda} \vec{v}. \quad (38)$$

However, it should be noted that the vector potential and Berry connection are gauge-dependent quantities, while the angular velocity is not typically tied to a specific gauge. Still, this difference between these two quantities may not be as well defined as one may think if we consider that a choice of gauge is ultimately associated with a choice of frame [90]. This aspect deserves to be further investigated since it is associated with a different discussion in the literature. On the one hand, in the nonrelativistic limit, the Sagnac effect can be seen as a manifestation of the lack of holonomy of the underlying geometry of the encircling particle, as we just showed — and previously argued by, e.g., Chiao [126] and Hendriks and Nienhuis [127]. As such, it is a Berry phase. On the other hand, this analogy between the Sagnac effect and AB effect or, more generally, Berry phases are not unanimous. For instance, while reviewing this effect, Malykin noted that Berry phases appear in addition to the Sagnac effect in different scenarios [128]. Moreover, the AB and Berry phases are related to quantum systems, while the Sagnac effect can be attributed to classical systems. Because of it, Malykin concludes that, although valid, the analogy with AB and Berry phases is not of a fundamental nature. In any case, the interplay between different geometric phases in different implementations of the Sagnac effect seems worthy of further exploration.

In the next section, we present various applications of the Sagnac effect in quantum metrology and sensing, with special emphasis on the detection of gravitational effects.

VI. APPLICATIONS OF THE SAGNAC INTERFEROMETER IN QUANTUM SENSING

In quantum sensing and metrology, one attempts to employ unique quantum properties such as single-particle interference, squeezing, and entanglement to improve classical techniques in terms of sensitivity, precision, or resolution. The probe particles could be massive or massless, but the goal in quantum metrology is typically to go beyond the shot-noise limit (SNL), towards the Heisenberg limit. For achieving this goal, interferometers traversed by quantum states of light or matter are known to be invaluable tools [129–135].

For utilizing uniquely quantum states, various methods have been suggested and implemented. For instance, in the case of optical interferometers, the preferred method for this purpose is the employment of quantum squeezing [136–138] due to the simple generation of squeezed light by parametric amplification and the ability to seed a standard, high-power classical interferometer with squeezed light. This method claims usufruct rights for both the quantum advantage of squeezing together and the classical advantage of power [139–141]. However, all sub-shot-noise methods require a high detection efficiency, greater than 90% for the SNL to be considerably overcome [138] and can be applied only in limited spectral ranges, where high-efficiency, low-noise detectors are available.

The Sagnac interferometer is a major interferometric tool of high scientific and technological importance that can also be enhanced by squeezing. The Sagnac is the basis of optical and matter-wave gyroscopes, which are critical for military and civilian applications. In addition, the zero-area Sagnac interferometer was suggested [134, 142, 143] for the next generation of gravitational wave detectors.

A. Quantum gyroscopes

Since the Sagnac interferometer is sensitive to rotations, a natural application that takes advantage of this characteristic is its use in the construction of gyroscopes. As such, this type of application became common since they were first suggested or implemented in optical [144–146] and matter-wave [147] setups. Assuming the Gödel metric, they were even proposed as a device capable of placing an upper bound on the rotation of the universe [122].

An important advantage of Sagnac interferometers over other configurations relies on their geometric nature. In fact, geometric phases depend exclusively on global

variables and are, thus, intrinsically immune to local noise disturbances that preserve these geometric features [30, 148]. Because of that, measurements of effects based on geometric phases can provide high-precision quantum sensing in real-world scenarios.

Here, we briefly present some advances in the development of Sagnac-based gyroscopes. To start, we focus on matter-wave gyroscopes. Since the first experimental application of the Sagnac effect with atoms [147], sensitivity improvements continued to be investigated [120, 149–151]. In particular, the use of trapped atoms was suggested [152–154] to overcome the complexity of implementing the atom gyroscopes [155]. Because they support the atoms against gravity, the traps present longer measurement times without requiring large dropping distances, which otherwise would be challenging for matter-waves. With that, configurations using trapped atomic clocks [148, 156] were shown to saturate the quantum Cramér-Rao bound. Moreover, entanglement-enhanced atomic gyroscopes with atoms trapped in an optical ring potential were proposed to achieve a precision of the order given by the Heisenberg limit [133].

On the optical side, it was first observed that single-mode fiber optic gyroscope had increased simplicity, stability, and the potential of very high rotation sensitivity [144–146]. However, the experiments began to really make use of quantum advantages after it was shown that the use of squeezed light in these gyroscopes could raise the sensitivity beyond the SNL [157, 158]. Entanglement was also shown to improve sensitivity in various schemes [159–161].

B. Third generation of gravitational wave detectors

Gravitational wave detectors have to meet harsh standards to function properly. For instance, in order to increase the information obtained from the measured interference pattern, they should use sophisticated feedback mechanisms allowing for major frequency and power stability. Moreover, they have to be extremely long to detect such small spacetime variations induced by gravitational waves. Also, like in most high-precision experiments with squeezed light, strict limits are imposed on the system's losses.

The Sagnac effect was suggested for detecting gravitational waves [115]. With that and envisioning it as a possible replacement to the Michelson-Fabry-Pérot-based LIGO, the zero-area Sagnac interferometer was introduced [162]. In this variation of the standard Sagnac interferometer, the waves still travel in opposite directions. However, the circuit is constructed in such a way to have area cancellation, as schematically illustrated in Figure 3. At first, it may seem that such an interferometer loses the most remarkable characteristic of the Sagnac interferometers: rotation sensitivity. However, some of the main advantages of this interferometer are its insensitivity to variations of laser frequency and its peak response

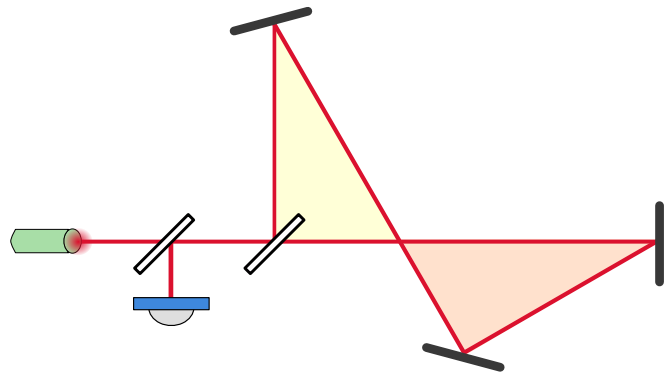


FIG. 3. **Schematic representation of a simple zero-area Sagnac interferometer.** The disjoint oriented areas enclosed by systems travelling the interferometer (in yellow and orange) cancel each other. As a result, such an interferometer is insensitive to rotations.

in the frequency band of interest for LIGO applications. Moreover, this interferometer is also insensitive to mirror displacement at dc, thermally induced birefringence, and reflectivity imbalance in the arms. With all that, the optical tolerance requirements of the system are reduced and the system is more easily controlled.

Nevertheless, these advantages did not suffice to overcome some of the Sagnac topology disadvantages, like its low tolerance to beamsplitter reflectivity error and beamsplitter tilt [163]. Furthermore, the ideal Sagnac interferometer did not present sensitivity advantages when compared to signal-recycled Michelson interferometers for the astrophysical needs of this type of application [164].

Despite these challenges, much effort was put into pushing the Sagnac scheme into an implementable state for the third generation of gravitational-wave detectors [134, 142, 143, 165–167]. For instance, it was shown that the zero-area Sagnac interferometer is a speedmeter, which can have advantages over position meters, like more conventional Michelson interferometers [143]. Moreover, the sensitivity of the zero-area Sagnac interferometer can be improved upon using ring cavities in the arms and signal recycling, similarly to the illustration in Figure 4 without the elements inside the area delimited by the dashed line, which were a later addition. Although this would make the sensibility of this interferometer and the Michelson scheme comparable, the implementation of the Sagnac device had the advantage of not requiring the addition of any extra Fabry-Pérot cavities.

Based on these results, it was suggested that further increase of the zero-area Sagnac interferometer's sensing could be achieved with the input of squeezed vacuum on its open port combined with a standard homodyne measurement [134]. However, such a measurement is inherently narrowband and requires near-ideal photodetectors as well as precise, technically demanding, active phase-locking of the squeezed vacuum to the local oscillator. Nevertheless, when compared to different interferometers, a Sagnac speedmeter is less susceptible to loss in

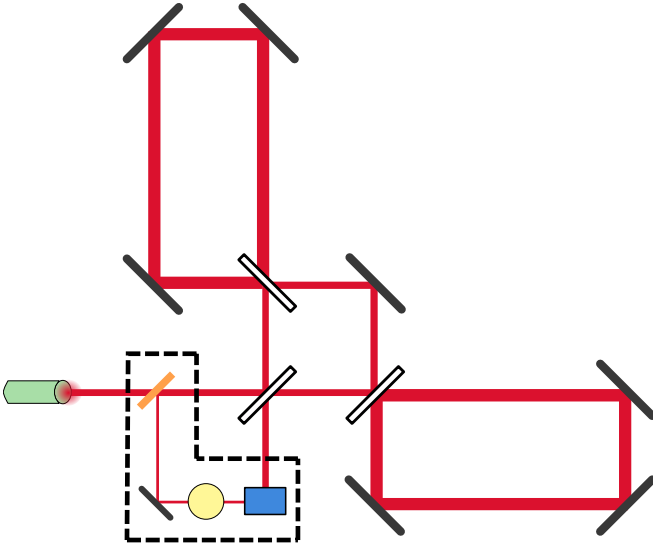


FIG. 4. **Schematic representation of the ring-Sagnac interferometer.** The inner Sagnac interferometer, composed of the three white beamsplitters and a mirror (black element), is attached to two resonant cavities, one attached to its top left and the other to its bottom right. The elements inside the area delimited by the dashed line are used for homodyne readout. The orange beamsplitter separates a small portion of the signal. Then, this portion is reflected by a mirror and goes through a phase shifter (yellow circle). The blue box represents a homodyne detector. This setup was analysed in Ref. [165].

a filter cavity [166]. This seems to firm the Sagnac topology as a good candidate for the third generation gravitational waves detectors since it simplifies the development of the filter cavity, reducing its implementation costs.

More improvements were suggested with the introduction of a sloshing-Sagnac interferometer, which is made out of two resonant Fabry-Pérot arm cavities in a Michelson configuration linked to a similar, antiresonant cavity running parallel to them [165]. This constitutes the Sagnac configuration represented in Figure 5. When compared to the ring-Sagnac interferometer shown in Figure 4, this device offers an extra degree of freedom for optimizations in the form of the finesse of the sloshing cavity that is separated from the arm cavity. In fact, with the use of squeezing, the sloshing-Sagnac interferometer presented a better performance in a lossy environment when compared to various other interferometers [167].

Before concluding this subsection and proceeding to a broader class of sensing techniques, it should be noted that alternatives to Sagnac interferometers are also being considered in the literature. For instance, Michelson interferometers can also be adapted to become speedmeters, which may give them some advantages compared to the more conventional Michelson interferometers [168–170].

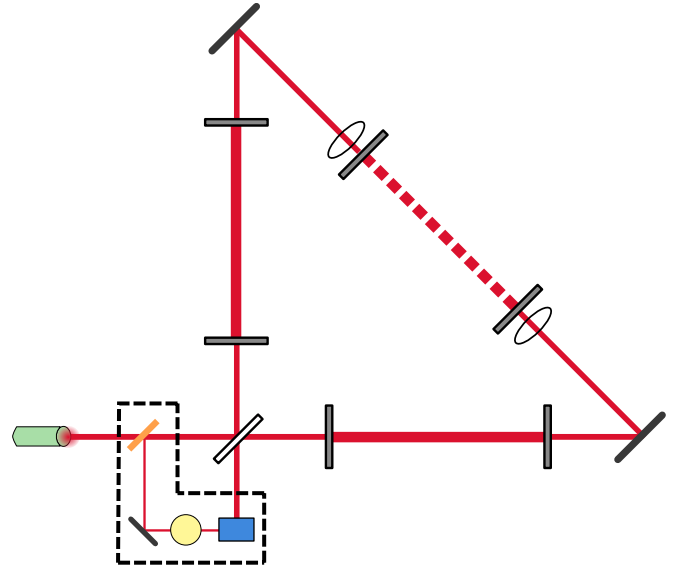


FIG. 5. **Schematic representation of the sloshing-Sagnac interferometer.** The main part of the interferometer is composed of a beamsplitter (white element) and the horizontal and vertical arms. In each arm, there are two mirrors with equal reflectance and transmittance (gray elements). The signal leaked at the end of each of these cavities is reflected by a mirror (black element) and linked to an antiresonant cavity (in the diagonal). Lenses, represented by the elliptical elements, are used to match the cavity modes. Finally, the elements inside the area delimited by the dashed line are used for homodyne readout, like in the ring-Sagnac interferometer. This setup was investigated in Ref. [165].

C. Enhanced sensing with weak value amplification

Weak value amplification [171–177] is a broad set of sensing techniques with diversified applications. It often consists of weakly coupling a quantum pointer to the quantum system of interest. The latter is pre- and post-selected, i.e., it has both initial and final boundary conditions $|\psi\rangle$ and $|\phi\rangle$, respectively. In this scenario, the shift of the pointer is, to first order in the coupling strength, proportional to the *weak value* [178]

$$A_w = \frac{\langle\phi|A|\psi\rangle}{\langle\phi|\psi\rangle} \quad (39)$$

of the measured operator A . As can be easily seen, the weak value of A is not confined to its spectrum and can thus be very large. This amplification was shown to be particularly helpful in the presence of technical noise and detector saturation [174, 177]. Related schemes use intermediate-strength or strong measurements for assessing weak values [179–182] or, alternatively, rely on the inverse weak values [183]. Weak values and weak measurements also bear interesting relations with the geometric phase [184–187].

Post-selection of the dark port of a Sagnac interferometer was shown to yield ultra-sensitive deflection [171] and

tilt measurements [183], as well as for sensitive gravimetry [188]. Another work used weak value amplification for improved sensing of angular rotations [189]. Enhancement of angular velocity measurements based on weak value amplification was recently demonstrated in Refs. [190, 191].

VII. AHARONOV-BOHM EFFECT AND NON-INERTIAL SYSTEMS

In this section, we discuss two effects that, to the best of our knowledge, have not been vastly considered in the literature and deserve more attention in practical applications.

From Larmor's theorem [192], it is known that a magnetic field B acting on a particle can be emulated by the rotation of the frame with an angular speed proportional to B . It could be asked, then, if this also holds in the case of the AB effect since the particle only travels in regions with a null field. This question was answered in 1973 by Aharonov and Carmi [193], and their solution was further studied and employed in Refs. [94, 124, 194]. They presented a direct analogy between the *vector potential* and the angular velocity. As a result, this analogy allows the understanding of the AB phase geometrically.

To understand the result presented by Aharonov and Carmi, consider a lab given by a narrow ring with an inner radius R_1 and an outer radius R_2 , as represented by the blue region in Figure 6. Also, assume that the ring rotates with an angular velocity ω and, for simplicity, that the ratio between the charge and mass is the same for every particle inside the ring. Moreover, the disc with radius R_1 is taken to be massive.

Because of its rotation, the ring experiences two pseudo-forces, namely the centrifugal and the Coriolis force. These forces, however, can be canceled by external electromagnetic forces. Indeed, the Coriolis force \vec{F}_C acting on an object with mass m and velocity \vec{v} (measured in the lab) can be written as $\vec{F}_C = m\vec{v} \times \vec{C}$, where \vec{C} is the field associated with \vec{F}_C . Moreover, because \vec{C} satisfies $\vec{\nabla} \cdot \vec{C} = 0$, \vec{F}_C is given by a field that is the rotation of a vector potential \vec{A}_C . Also, if \vec{F}_c is the centrifugal force, $\vec{\nabla} \times \vec{F}_c = 0$, i.e., \vec{F}_c can be written as the gradient of a scalar potential.

Then, suppose an electromagnetic field is applied only *inside* the ring to remove the pseudo-forces. Even in this case, a quantum experiment with a particle enclosing the disk D_1 (with radius R_1) in a superposition of wavepackets traveling in different paths, as represented in Figure 6, can detect that the ring is not an inertial frame. In fact, denoting by \vec{A}_T the vector potential associated with the rotating mass after the inclusion of the magnetic field in the lab, it is possible to write the Hamiltonian of the system as

$$H = \frac{1}{2m} \left(\vec{P} - m\vec{A}_T \right)^2, \quad (40)$$

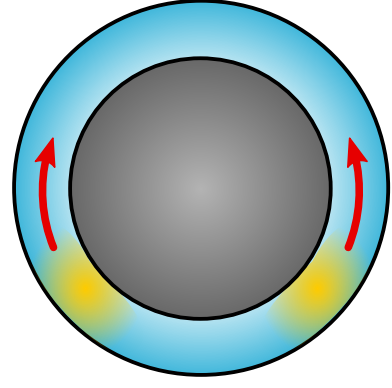


FIG. 6. **Representation of a laboratory given by a narrow ring.** The massive disk (gray circle) and the laboratory (blue region) are assumed to rotate as a single system. Even if an electromagnetic field is used to counterbalance the gravitational field generated by the massive disk and the fictitious force created by its rotation inside the laboratory, a quantum experiment can still detect that the laboratory is not an inertial frame.

which implies that the relative phase accumulated by the wavepackets is proportional to

$$\Delta\phi_R = m \oint \vec{A}_T \cdot d\vec{\ell} = m \int_{D_1} \vec{C} \cdot d\vec{S} = 2\pi m R_1^2 \omega, \quad (41)$$

i.e., the accumulated phase is proportional to the angular speed ω of the lab. The Hamiltonian in Eq. (40) compares to the Hamiltonian associated with the AB effect in Eq. (23). Moreover, a computation similar to the one performed in Eq. (30) shows that $\Delta\phi_R$ is indeed a geometric phase.

This phenomenon is an AB-like effect. It suggests the necessity for a modification of the equivalence principle in quantum theories. In fact, the charge travels in regions where the effective field is null, although its potential is not. In particular, we can deduce from the previous example that, in a general relativistic treatment, curvature effects, and not just accelerations caused by them, can be detected in quantum interference experiments. Indeed, low-order curvature effects were studied in an interferometer with thermal neutrons that only makes use of horizontal mirrors [195].

Moreover, another similarity between the example studied in this section and the magnetic AB effect is that the trajectories of the wavepackets can be deformed and, as long as they do not enter the gray region in Figure 6, the acquired relative phase between them is unchanged. However, differently from the magnetic AB effect, the phase considered here is acquired in a manifestly local manner.

One can go even further and discuss the gravitational AB effect [196–200]. In particular, the authors of Ref. [200] replace the magnetic flux with a Lense-Thirring field. Then, they show a relation between this effect and gravitational radiation and parametric oscillators. Generally speaking, it seems that the gravitational

AB effect may enjoy the better sensitivity of the proposed squeezing-enhanced Sagnac interferometer. However, this is a practical question that deserves further exploration.

VIII. DISCUSSION AND OUTLOOK

The geometry of quantum states is remarkable in breadth and depth. We have only described a small selection of its various fundamental and practical merits in this review article. On the fundamental side, it arises from a rich mathematical structure that can be related to a classical counterpart via the Bohr-Sommerfeld quantization rule, as we explained briefly in Section III. Moreover, AB-like non-inertial and gravitational effects introduce interesting quantum phenomena and even suggest the necessity of a reformulation of basic concepts, like the equivalence principle, as seen in Section VII. On the application side, particular attention was given to gravitational and non-inertial measurements. However, geometric phases are also an important player in quantum information and computation [201–203], chemical physics [5, 21, 204, 205], and many other areas.

Before concluding, we outline some topics for further research. From a practical perspective, the geometric and gravitational AB effects do not seem to be vastly studied in the literature and may lead to new quantum-enhanced precision measurements. These effects and their relation to other relativistic ones, such as frame-dragging, seem to deserve further attention.

On the fundamental level, there are still some open questions such as: Does the analogy between various geometric phases and the Sagnac effect represent a genuine physical relation between them? Is the AB effect local? If so, in which sense? Can constructions of a complete quantum mechanical description of systems which does not utilize potentials help in this investigation?

Regarding this last question, it indeed seems that

an interesting direction is the study of fully quantized systems where gauge-dependence is linked to frame-dependence [90, 101]. This approach could reveal similarities and also highlight important differences between the AB and other geometric phases.

In this approach and other similar ones, geometric and topological phases were linked to the creation of entanglement. For instance, in the case of the AB effect, if the source of the magnetic field is not an eigenstate of a relevant observable, the source and the charge encircling it become entangled [101]. However, as argued by Vaidman [93], it is possible to conceive a model in which entanglement is present even if initially there is no uncertainty in the flux. This suggests that a general interplay may exist between dynamical nonlocality and kinematical nonlocality (see also [98]). The latter is a broad category that includes, for instance, Bell nonlocality. The former is a type of nonlocality that emerges from the dynamical equations of motion [60, 72, 206] and can be associated, e.g., with the AB effect. Then, a better understanding of how entanglement is related to these phases could have fundamental and practical consequences.

Finally, one may also study to what extent other effects associated with geometric phases, like the optical Magnus effect [207–211], are fundamentally related or can benefit from the Sagnac effect.

ACKNOWLEDGMENTS

We thank Ady Arie, Avi Pe’er, and Michael Rosenbluh for many helpful discussions. This research was supported by grant number FQXi-RFP-CPW-2006 from the Foundational Questions Institute and Fetzer Franklin Fund, a donor-advised fund of Silicon Valley Community Foundation, by the Israeli Innovation authority (grants 70002 and 73795), by the Pazy foundation, and by the Quantum Science and Technology Program of the Israeli Council of Higher Education.

-
- [1] M. V. Berry, Quantal phase factors accompanying adiabatic changes, *Proc. R. Soc. Lond. A* **392**, 45 (1984).
 - [2] M. Berry, The geometric phase, *Sci. Am.* **259**, 46 (1988).
 - [3] A. Shapere and F. Wilczek, *Geometric phases in physics*, Advanced Series in Mathematical Physics, Vol. 5 (World Scientific, Singapore, 1989).
 - [4] S. S. Olariu and I. I. Popescu, The quantum effects of electromagnetic fluxes, *Rev. Mod. Phys.* **57**, 339 (1985).
 - [5] J. W. Zwanziger, M. Koenig, and A. Pines, Berry’s phase, *Annu. Rev. Phys. Chem.* **41**, 601 (1990).
 - [6] J. Anandan, The geometric phase, *Nature* **360**, 307 (1992).
 - [7] E. Cohen, H. Larocque, F. Bouchard, F. Nejadsattari, Y. Gefen, and E. Karimi, Geometric phase from Aharonov-Bohm to Pancharatnam-Berry and beyond, *Nat. Rev. Phys.* **1**, 437 (2019).
 - [8] A. Karnieli, Y. Li, and A. Arie, The geometric phase in nonlinear frequency conversion, *Front. Phys.* **17**, 12301 (2022).
 - [9] E. J. Post, Sagnac effect, *Rev. Mod. Phys.* **39**, 475 (1967).
 - [10] R. Anderson, H. R. Bilger, and G. E. Stedman, “Sagnac” effect: A century of Earth-rotated interferometers, *Am. J. Phys.* **62**, 975 (1994).
 - [11] K. U. Schreiber and J.-P. R. Wells, Invited review article: Large ring lasers for rotation sensing, *Rev. Sci. Instrum.* **84**, 041101 (2013).
 - [12] J. E. Marsden, R. Montgomery, and T. S. Ratiu, *Reduction, Symmetry, and Phases in Mechanics*, Memoirs of the American Mathematical Society No. 436 (AMS, Providence, RI, 1990).
 - [13] D. Chruściński and A. Jamiolkowski, *Geometric Phases in Classical and Quantum Mechanics*, Progress in Mathematical Physics, Vol. 36 (Birkhäuser, Boston, MA,

- 2004).
- [14] J. Anandan and Y. Aharonov, Geometry of quantum evolution, *Phys. Rev. Lett.* **65**, 1697 (1990).
 - [15] A. C. Lobo, R. A. Ribeiro, C. de Assis Ribeiro, and P. R. Dieguez, Geometry of the adiabatic theorem, *Eur. J. Phys.* **33**, 1063 (2012).
 - [16] I. L. Paiva, *Alguns Aspectos do Tempo na Mecânica Quântica*, Master's thesis, Universidade Federal de Minas Gerais (2014).
 - [17] S. Tamate, H. Kobayashi, T. Nakanishi, K. Sugiyama, and M. Kitano, Geometrical aspects of weak measurements and quantum erasers, *New J. Phys.* **11**, 093025 (2009).
 - [18] A. C. Lobo, Y. Aharonov, J. Tollaksen, E. M. Berri-gan, and C. de Assis Ribeiro, Weak values and modular variables from a quantum phase-space perspective, *Quantum Studies: Math. Found.* **1**, 97 (2014).
 - [19] B. Simon, Holonomy, the quantum adiabatic theorem, and Berry's phase, *Phys. Rev. Lett.* **51**, 2167 (1983).
 - [20] Y. Aharonov and J. Anandan, Phase change during a cyclic quantum evolution, *Phys. Rev. Lett.* **58**, 1593 (1987).
 - [21] C. A. Mead, The geometric phase in molecular systems, *Rev. Mod. Phys.* **64**, 51 (1992).
 - [22] R. Resta, Macroscopic polarization in crystalline dielectrics: the geometric phase approach, *Rev. Mod. Phys.* **66**, 899 (1994).
 - [23] E. Sjöqvist, A. K. Pati, A. Ekert, J. S. Anandan, M. Ericsson, D. K. Oi, and V. Vedral, Geometric phases for mixed states in interferometry, *Phys. Rev. Lett.* **85**, 2845 (2000).
 - [24] K. Singh, D. M. Tong, K. Basu, J. L. Chen, and J. F. Du, Geometric phases for nondegenerate and degenerate mixed states, *Phys. Rev. A* **67**, 032106 (2003).
 - [25] J. C. Garrison and E. M. Wright, Complex geometrical phases for dissipative systems, *Phys. Lett. A* **128**, 177 (1988).
 - [26] M. V. Berry, Geometric amplitude factors in adiabatic quantum transitions, *Proc. R. Soc. Lond. A Math. Phys. Sci.* **430**, 405 (1990).
 - [27] J. W. Zwanziger, S. P. Rucker, and G. C. Chingas, Measuring the geometric component of the transition probability in a two-level system, *Phys. Rev. A* **43**, 3232 (1991).
 - [28] C.-Z. Ning and H. Haken, Geometrical phase and amplitude accumulations in dissipative systems with cyclic attractors, *Phys. Rev. Lett.* **68**, 2109 (1992).
 - [29] K. Y. Bliokh, The appearance of a geometric-type instability in dynamic systems with adiabatically varying parameters, *J. Phys. A* **32**, 2551 (1999).
 - [30] A. Carollo, I. Fuentes-Guridi, M. F. Santos, and V. Vedral, Geometric phase in open systems, *Phys. Rev. Lett.* **90**, 160402 (2003).
 - [31] D. M. Tong, E. Sjöqvist, L. C. Kwek, and C. H. Oh, Kinematic approach to the mixed state geometric phase in nonunitary evolution, *Phys. Rev. Lett.* **93**, 080405 (2004).
 - [32] F. C. Lombardo and P. I. Villar, Geometric phases in open systems: A model to study how they are corrected by decoherence, *Phys. Rev. A* **74**, 042311 (2006).
 - [33] B. Dietz, H. L. Harney, O. N. Kirillov, M. Miski-Oglu, A. Richter, and F. Schäfer, Exceptional points in a microwave billiard with time-reversal invariance violation, *Phys. Rev. Lett.* **106**, 150403 (2011).
 - [34] Z. Wu and J. Wang, Berry's phase and Aharonov-Anandan's phase, *Physica A* **232**, 201 (1996).
 - [35] J. Samuel and R. Bhandari, General setting for Berry's phase, *Phys. Rev. Lett.* **60**, 2339 (1988).
 - [36] J. H. Hannay, Angle variable holonomy in adiabatic excursion of an integrable Hamiltonian, *J. Phys. A* **18**, 221 (1985).
 - [37] V. I. Arnol'd, *Mathematical Methods of Classical Mechanics* (Springer-Verlag, New York, NY, 1989).
 - [38] S. Golin, A. Knauf, and S. Marmi, The Hannay angles: geometry, adiabaticity, and an example, *Commun. Math. Phys.* **123**, 95 (1989).
 - [39] A. K. Pati, Adiabatic Berry phase and Hannay angle for open paths, *Ann. Phys.* **270**, 178 (1998).
 - [40] T. B. Kepler and M. L. Kagan, Geometric phase shifts under adiabatic parameter changes in classical dissipative systems, *Phys. Rev. Lett.* **66**, 847 (1991).
 - [41] S. B. Andersson, Nonadiabatic corrections to the Hannay-Berry phase, *SIAM J. Appl. Math.* **66**, 98 (2005).
 - [42] J. C. Garrison and R. Y. Chiao, Geometrical phases from global gauge invariance of nonlinear classical field theories, *Phys. Rev. Lett.* **60**, 165 (1988).
 - [43] J. Anandan, Comment on geometric phases for classical field theories, *Phys. Rev. Lett.* **60**, 2555 (1988).
 - [44] L. Latmiral and F. Armata, Berry-Hannay relation in nonlinear optomechanics, *Sci. Rep.* **10**, 2264 (2020).
 - [45] M. V. Berry, Classical adiabatic angles and quantal adiabatic phase, *J. Phys. A* **18**, 15 (1985).
 - [46] F. Armata, L. Latmiral, I. Pikovski, M. R. Vanner, Č. Brukner, and M. Kim, Quantum and classical phases in optomechanics, *Phys. Rev. A* **93**, 063862 (2016).
 - [47] G. S. Agarwal and R. Simon, Berry phase, interference of light beams, and the Hannay angle, *Phys. Rev. A* **42**, 6924 (1990).
 - [48] S. Chaturvedi, M. S. Sriram, and V. Srinivasan, Berry's phase for coherent states, *J. Phys. A* **20**, L1071 (1987).
 - [49] R. Y. Chiao and T. F. Jordan, Lorentz-group Berry phases in squeezed light, *Phys. Lett. A* **132**, 77 (1988).
 - [50] I. Fuentes-Guridi, S. Bose, and V. Vedral, Proposal for measurement of harmonic oscillator Berry phase in ion traps, *Phys. Rev. Lett.* **85**, 5018 (2000).
 - [51] F. Wilczek and A. Zee, Appearance of gauge structure in simple dynamical systems, *Phys. Rev. Lett.* **52**, 2111 (1984).
 - [52] J. Anandan, Non-adiabatic non-abelian geometric phase, *Phys. Lett. A* **133**, 171 (1988).
 - [53] W. Franz, Elektroneninterferenzen im Magnetfeld, *Verh. Dtsch. Phys. Ges.* **20**, 65 (1939).
 - [54] W. Ehrenberg and R. E. Siday, The refractive index in electron optics and the principles of dynamics, *Proc. Phys. Soc. B* **62**, 8 (1949).
 - [55] Y. Aharonov and D. Bohm, Significance of electromagnetic potentials in the quantum theory, *Phys. Rev.* **115**, 485 (1959).
 - [56] B. J. Hiley, The early history of the Aharonov-Bohm effect, *arXiv:1304.4736* (2013).
 - [57] R. G. Chambers, Shift of an electron interference pattern by enclosed magnetic flux, *Phys. Rev. Lett.* **5**, 3 (1960).
 - [58] G. Möllenstedt and W. Bayh, Kontinuierliche Phasenschiebung von Elektronenwellen im kraftfeldfreien Raum durch das magnetische Vektorpotential eines Solenoids, *Phys. Blätter* **18**, 299 (1962).

- [59] B. Liebowitz, Significance of the Aharonov-Bohm effect, *Il Nuovo Cimento* **38**, 932 (1965).
- [60] Y. Aharonov, H. Pendleton, and A. Petersen, Modular variables in quantum theory, *Int. J. Theor. Phys.* **2**, 213 (1969).
- [61] T. H. Boyer, Classical electromagnetic deflections and lag effects associated with quantum interference pattern shifts: Considerations related to the Aharonov-Bohm effect, *Phys. Rev. D* **8**, 1679 (1973).
- [62] M. V. Berry, R. G. Chambers, M. D. Large, C. Upstill, and J. C. Walmsley, Wavefront dislocations in the Aharonov-Bohm effect and its water wave analogue, *Eur. J. Phys.* **1**, 154 (1980).
- [63] A. Tonomura, T. Matsuda, R. Suzuki, A. Fukuhara, N. Osakabe, H. Umezaki, J. Endo, K. Shinagawa, Y. Sugita, and H. Fujiwara, Observation of Aharonov-Bohm effect by electron holography, *Phys. Rev. Lett.* **48**, 1443 (1982).
- [64] A. Tonomura, N. Osakabe, T. Matsuda, T. Kawasaki, J. Endo, S. Yano, and H. Yamada, Evidence for Aharonov-Bohm effect with magnetic field completely shielded from electron wave, *Phys. Rev. Lett.* **56**, 792 (1986).
- [65] M. Berry, The Aharonov-Bohm effect is real physics not ideal physics, in *Fundamental Aspects of Quantum Theory*, Nato Science Series B, Vol. 144, edited by V. Gorini and A. Frigerio (Springer, New York, 1986) p. 319.
- [66] M. V. Berry and M. Robnik, Statistics of energy levels without time-reversal symmetry: Aharonov-Bohm chaotic billiards, *J. Phys. A: Math. Gen.* **19**, 649 (1986).
- [67] N. Osakabe, T. Matsuda, T. Kawasaki, J. Endo, A. Tonomura, S. Yano, and H. Yamada, Experimental confirmation of Aharonov-Bohm effect using a toroidal magnetic field confined by a superconductor, *Phys. Rev. A* **34**, 815 (1986).
- [68] M. Berry, Quantum chaology, not quantum chaos, *Phys. Scr.* **40**, 335 (1989).
- [69] C. J. B. Ford, P. J. Simpson, I. Zailer, J. D. F. Franklin, C. H. W. Barnes, J. E. F. Frost, D. A. Ritchie, and M. Pepper, The Aharonov-Bohm effect in the fractional quantum Hall regime, *J. Phys.: Cond. Matt.* **6**, L725 (1994).
- [70] Y. Aharonov, S. Coleman, A. S. Goldhaber, S. Nussinov, S. Popescu, B. Reznik, D. Rohrlich, and L. Vaidman, Aharonov-Bohm and Berry phases for a quantum cloud of charge, *Phys. Rev. Lett.* **73**, 918 (1994).
- [71] Y. Aharonov and T. Kaufherr, The effect of a magnetic flux line in quantum theory, *Phys. Rev. Lett.* **92**, 070404 (2004).
- [72] Y. Aharonov and D. Rohrlich, *Quantum Paradoxes: Quantum Theory for the Perplexed* (Wiley-VCH, Weinheim, 2005).
- [73] A. Tonomura, The Aharonov-Bohm effect and its applications to electron phase microscopy, *Proc. Jpn. Acad. Ser. B: Phys. Biol. Sci.* **82**, 45 (2006).
- [74] P. Recher, B. Trauzettel, A. Rycerz, Y. M. Blanter, C. W. J. Beenakker, and A. F. Morpurgo, Aharonov-Bohm effect and broken valley degeneracy in graphene rings, *Phys. Rev. B* **76**, 235404 (2007).
- [75] S. Russo, J. B. Oostinga, D. Wehenkel, H. B. Heersche, S. S. Sobhani, L. M. K. Vandersypen, and A. F. Morpurgo, Observation of Aharonov-Bohm conductance oscillations in a graphene ring, *Phys. Rev. B* **77**, 085413 (2008).
- [76] H. Peng, K. Lai, D. Kong, S. Meister, Y. Chen, X.-L. Qi, S.-C. Zhang, Z.-X. Shen, and Y. Cui, Aharonov-Bohm interference in topological insulator nanoribbons, *Nat. Mat.* **9**, 225 (2010).
- [77] M. V. Berry and S. Popescu, Semifluxon degeneracy choreography in Aharonov-Bohm billiards, *J. Phys. A: Math. Theor.* **43**, 354005 (2010).
- [78] K. Fang, Z. Yu, and S. Fan, Photonic Aharonov-Bohm effect based on dynamic modulation, *Phys. Rev. Lett.* **108**, 153901 (2012).
- [79] J. H. Bardarson and J. E. Moore, Quantum interference and Aharonov-Bohm oscillations in topological insulators, *Rep. Prog. Phys.* **76**, 056501 (2013).
- [80] A. Noguchi, Y. Shikano, K. Toyoda, and S. Urabe, Aharonov-Bohm effect in the tunneling of a quantum rotor in a linear Paul trap, *Nat. Commun.* **5**, 3868 (2014).
- [81] L. Duca, T. Li, M. Reitter, I. Bloch, M. Schleier-Smith, and U. Schneider, An Aharonov-Bohm interferometer for determining Bloch band topology, *Science* **347**, 288 (2015).
- [82] K. Kang, Locality of the Aharonov-Bohm-Casher effect, *Phys. Rev. A* **91**, 052116 (2015).
- [83] E. Cohen, L. Vaidman, and Y. Aharonov, How to measure magnetic flux with a single position measurement?, *Europhys. Lett.* **110**, 50004 (2015).
- [84] Y. Aharonov, E. Cohen, and D. Rohrlich, Nonlocality of the Aharonov-Bohm effect, *Phys. Rev. A* **93**, 042110 (2016).
- [85] S. Mukherjee, M. Di Liberto, P. Öhberg, R. R. Thomson, and N. Goldman, Experimental observation of Aharonov-Bohm cages in photonic lattices, *Phys. Rev. Lett.* **121**, 075502 (2018).
- [86] I. L. Paiva, Y. Aharonov, J. Tollaksen, and M. Waegell, Topological bound states for quantum charges, *Phys. Rev. A* **100**, 040101 (2019).
- [87] I. L. Paiva, Y. Aharonov, J. Tollaksen, and M. Waegell, Magnetic forces in the absence of a classical magnetic field, *Phys. Rev. A* **101**, 042111 (2020).
- [88] P. A. M. Dirac, Quantised singularities in the electromagnetic field, *Proc. R. Soc. Lond. A* **133**, 60 (1931).
- [89] M. Peshkin, I. Talmi, and L. J. Tassie, The quantum mechanical effects of magnetic fields confined to inaccessible regions, *Ann. Phys.* **12**, 426 (1961).
- [90] Y. Aharonov and J. Anandan, Is there a preferred canonical quantum gauge?, *Phys. Lett. A* **160**, 493 (1991).
- [91] E. Santos and I. Gonzalo, Microscopic theory of the Aharonov-Bohm effect, *Europhys. Lett.* **45**, 418 (1999).
- [92] M. Y. Choi and M. Lee, Exact quantum description of the Aharonov-Bohm effect, *Curr. Appl. Phys.* **4**, 267 (2004).
- [93] L. Vaidman, Role of potentials in the Aharonov-Bohm effect, *Phys. Rev. A* **86**, 040101(R) (2012).
- [94] Y. Aharonov, E. Cohen, and D. Rohrlich, Comment on “Role of potentials in the Aharonov-Bohm effect”, *Phys. Rev. A* **92**, 026101 (2015).
- [95] L. Vaidman, Reply to “Comment on ‘Role of potentials in the Aharonov-Bohm effect’”, *Phys. Rev. A* **92**, 026102 (2015).
- [96] P. Pearle and A. Rizzi, Quantized vector potential and alternative views of the magnetic Aharonov-Bohm phase shift, *Phys. Rev. A* **95**, 052124 (2017).
- [97] B. Li, D. W. Hewak, and Q. J. Wang, The transi-

- tion from quantum field theory to one-particle quantum mechanics and a proposed interpretation of Aharonov-Bohm effect, *Found. Phys.* **48**, 837 (2018).
- [98] C. Marletto and V. Vedral, Aharonov-Bohm phase is locally generated like all other quantum phases, *Phys. Rev. Lett.* **125**, 040401 (2020).
 - [99] P. L. Saldanha, C. Marletto, and V. Vedral, Shielded, local Aharonov-Bohm effects: how quantum phases cannot be stopped, [arXiv:2011.09005](#) (2020).
 - [100] S. Horvat, P. A. Guérin, L. Apadula, and F. Del Santo, Probing quantum coherence at a distance and Aharonov-Bohm nonlocality, *Phys. Rev. A* **102**, 062214 (2020).
 - [101] I. L. Paiva, Y. Aharonov, J. Tollaksen, and M. Waegell, Aharonov-Bohm effect with an effective complex-valued vector potential, [arXiv:2101.11914](#) (2021).
 - [102] Y. Aharonov, S. Coleman, A. S. Goldhaber, S. Nussinov, S. Popescu, B. Reznik, D. Rohrlich, and L. Vaidman, Aharonov-Bohm and Berry phases for a quantum cloud of charge, *Phys. Rev. Lett.* **73**, 918 (1994).
 - [103] Y. Aharonov and A. Casher, Topological quantum effects for neutral particles, *Phys. Rev. Lett.* **53**, 319 (1984).
 - [104] H. Kaiser, M. Arif, R. Berliner, R. Clothier, S. A. Werner, A. Cimmino, A. G. Klein, and G. I. Opat, Neutron interferometry investigation of the Aharonov-Casher effect, *Physica B+C* **151**, 68 (1988).
 - [105] A. S. Goldhaber, Comment on “Topological quantum effects for neutral particles”, *Phys. Rev. Lett.* **62**, 482 (1989).
 - [106] A. Cimmino, G. I. Opat, A. G. Klein, H. Kaiser, S. A. Werner, M. Arif, and R. Clothier, Observation of the topological Aharonov-Casher phase shift by neutron interferometry, *Phys. Rev. Lett.* **63**, 380 (1989).
 - [107] J. Dalibard, F. Gerbier, G. Juzeliūnas, and P. Öhberg, Colloquium: Artificial gauge potentials for neutral atoms, *Rev. Mod. Phys.* **83**, 1523 (2011).
 - [108] G. Sagnac, Sur la preuve de la réalité de l'éther lumineux par l'expérience de l'interférographe tournant, *C. R. Acad. Sci.* **157**, 708 (1913).
 - [109] O. J. Lodge, XV. Aberration problems. A discussion concerning the motion of the ether near the earth, and concerning the connexion between ether and gross matter; with some new experiments, *Philos. Trans. R. Soc. Lond. A*, 727 (1893).
 - [110] O. J. Lodge, Vi. experiments on the absence of mechanical connexion between ether and matter, *Philos. Trans. R. Soc. of Lond. A*, 149 (1897).
 - [111] A. A. Michelson and H. G. Gale, The effect of the Earth's rotation on the velocity of light, Part II, *Astrophys. J.* **61**, 140 (1925).
 - [112] R. Colella, A. W. Overhauser, and S. A. Werner, Observation of gravitationally induced quantum interference, *Phys. Rev. Lett.* **34**, 1472 (1975).
 - [113] A. W. Overhauser and R. Colella, Experimental test of gravitationally induced quantum interference, *Phys. Rev. Lett.* **33**, 1237 (1974).
 - [114] S. A. Werner, J.-L. Staudenmann, and R. Colella, Effect of Earth's rotation on the quantum mechanical phase of the neutron, *Phys. Rev. Lett.* **42**, 1103 (1979).
 - [115] J. Anandan, Sagnac effect in relativistic and nonrelativistic physics, *Phys. Rev. D* **24**, 338 (1981).
 - [116] J. Frauendiener, Notes on the Sagnac effect in general relativity, *Gen. Relativ. Gravit.* **50**, 147 (2018).
 - [117] J. Frauendiener, Gravitational waves and the Sagnac effect, *Class. Quantum Grav.* **37**, 05LT01 (2020).
 - [118] A. Tartaglia and M. L. Ruggiero, The Sagnac effect and pure geometry, *Am. J. Phys.* **83**, 427 (2015).
 - [119] F. Hasselbach and M. Nicklaus, Sagnac experiment with electrons: Observation of the rotational phase shift of electron waves in vacuum, *Phys. Rev. A* **48**, 143 (1993).
 - [120] T. L. Gustavson, P. Bouyer, and M. A. Kasevich, Precision rotation measurements with an atom interferometer gyroscope, *Phys. Rev. Lett.* **78**, 2046 (1997).
 - [121] J. Anandan, Gravitational and inertial effects in quantum fluids, *Phys. Rev. Lett.* **47**, 463 (1981); Errata: Gravitational and inertial effects in quantum fluids, *Phys. Rev. Lett.* **52**, 401 (1984).
 - [122] A. Delgado, W. P. Schleich, and G. Süssmann, Quantum gyroscopes and Gödel's universe: entanglement opens a new testing ground for cosmology, *New J. Phys.* **4**, 37 (2002).
 - [123] B. Barrett, R. Geiger, I. Dutta, M. Meunier, B. Canuel, A. Gauguier, P. Bouyer, and A. Landragin, The Sagnac effect: 20 years of development in matter-wave interferometry, *C. R. Phys.* **15**, 875 (2014).
 - [124] Y. Aharonov and E. Cohen, How to measure magnetic flux with a single position measurement, [arXiv:1408.5871](#) (2014).
 - [125] R. Wang, Y. Zheng, and A. Yao, Generalized Sagnac effect, *Phys. Rev. Lett.* **93**, 143901 (2004).
 - [126] R. Chiao, Berry's phases in optics: Aharonov-Bohm-like effects and gauge structures in surprising contexts, *Nucl. Phys. B: Proc. Suppl.* **6**, 298 (1989).
 - [127] B. Hendricks and G. Nienhuis, Sagnac effect as viewed by a co-rotating observer, *Quantum Opt.* **2**, 13 (1990).
 - [128] G. B. Malykin, The Sagnac effect: correct and incorrect explanations, *Phys.-Usp.* **43**, 1229 (2000).
 - [129] V. Giovannetti, S. Lloyd, and L. Maccone, Quantum-enhanced measurements: beating the standard quantum limit, *Science* **306**, 1330 (2004).
 - [130] M. W. Mitchell, J. S. Lundeen, and A. M. Steinberg, Super-resolving phase measurements with a multiphoton entangled state, *Nature* **429**, 161 (2004).
 - [131] T. Nagata, R. Okamoto, J. L. O'Brien, K. Sasaki, and S. Takeuchi, Beating the standard quantum limit with four-entangled photons, *Science* **316**, 726 (2007).
 - [132] K. J. Resch, K. L. Pagnell, R. Prevedel, A. Gilchrist, G. J. Pryde, J. L. O'Brien, and A. G. White, Time-reversal and super-resolving phase measurements, *Phys. Rev. Lett.* **98**, 223601 (2007).
 - [133] J. J. Cooper, D. W. Hallwood, and J. A. Dunningham, Entanglement-enhanced atomic gyroscope, *Phys. Rev. A* **81**, 043624 (2010).
 - [134] T. Eberle, S. Steinlechner, J. Bauchrowitz, V. Händchen, H. Vahlbruch, M. Mehmet, H. Müller-Ebhardt, and R. Schnabel, Quantum enhancement of the zero-area Sagnac interferometer topology for gravitational wave detection, *Phys. Rev. Lett.* **104**, 251102 (2010).
 - [135] F. Wolf, C. Shi, J. C. Heip, M. Gessner, L. Pezzè, A. Smerzi, M. Schulte, K. Hammerer, and P. O. Schmidt, Motional Fock states for quantum-enhanced amplitude and phase measurements with trapped ions, *Nat. Commun.* **10**, 2929 (2019).
 - [136] C. M. Caves, Quantum-mechanical noise in an interferometer, *Phys. Rev. D* **23**, 1693 (1981).

- [137] M. Xiao, L.-A. Wu, and H. J. Kimble, Precision measurement beyond the shot-noise limit, *Phys. Rev. Lett.* **59**, 278 (1987).
- [138] R. Schnabel, Squeezed states of light and their applications in laser interferometers, *Phys. Rep.* **684**, 1 (2017).
- [139] The LIGO Scientific Collaboration, A gravitational wave observatory operating beyond the quantum shot-noise limit, *Nat. Phys.* **7**, 962 (2011).
- [140] L. Barsotti, J. Harms, and R. Schnabel, Squeezed vacuum states of light for gravitational wave detectors, *Rep. Prog. Phys.* **82**, 016905 (2018).
- [141] M. Tse *et al.*, Quantum-enhanced advanced LIGO detectors in the era of gravitational-wave astronomy, *Phys. Rev. Lett.* **123**, 231107 (2019).
- [142] S. Traeger, P. Beyersdorf, L. Goddard, E. Gustafson, M. M. Fejer, and R. L. Byer, Polarization Sagnac interferometer with a reflective grating beam splitter, *Opt. Lett.* **25**, 722 (2000).
- [143] Y. Chen, Sagnac interferometer as a speed-meter-type, quantum-nondemolition gravitational-wave detector, *Phys. Rev. D* **67**, 122004 (2003).
- [144] V. Vali and R. W. Shorthill, Fiber laser gyroscopes, in *Fibers and Integrated Optics*, Vol. 77, International Society for Optics and Photonics (SPIE, 1976) pp. 110–115.
- [145] R. A. Bergh, H. C. Lefevre, and H. J. Shaw, All-single-mode fiber-optic gyroscope, *Opt. Lett.* **6**, 198 (1981).
- [146] R. A. Bergh, H. C. Lefevre, and H. J. Shaw, All-single-mode fiber-optic gyroscope with long-term stability, *Opt. Lett.* **6**, 502 (1981).
- [147] F. Riehle, T. Kisters, A. Witte, J. Helmcke, and C. J. Bordé, Optical Ramsey spectroscopy in a rotating frame: Sagnac effect in a matter-wave interferometer, *Phys. Rev. Lett.* **67**, 177 (1991).
- [148] Y. Che, F. Yao, H. Liang, G. Li, and X. Wang, Phase-space geometric Sagnac interferometer for rotation sensing, *Phys. Rev. A* **98**, 053609 (2018).
- [149] J. P. Dowling, Correlated input-port, matter-wave interferometer: Quantum-noise limits to the atom-laser gyroscope, *Phys. Rev. A* **57**, 4736 (1998).
- [150] T. L. Gustavson, A. Landragin, and M. A. Kasevich, Rotation sensing with a dual atom-interferometer Sagnac gyroscope, *Class. Quantum Gravity* **17**, 2385 (2000).
- [151] S. Wu, E. Su, and M. Prentiss, Demonstration of an area-enclosing guided-atom interferometer for rotation sensing, *Phys. Rev. Lett.* **99**, 173201 (2007).
- [152] W. Ketterle and D. E. Pritchard, Trapping and focusing ground state atoms with static fields, *Appl. Phys. B* **54**, 403 (1992).
- [153] J. A. Sauer, M. D. Barrett, and M. S. Chapman, Storage ring for neutral atoms, *Phys. Rev. Lett.* **87**, 270401 (2001).
- [154] A. S. Arnold, Adaptable-radius, time-orbiting magnetic ring trap for Bose-Einstein condensates, *J. Phys. B* **37**, L29 (2003).
- [155] E. R. Moan, R. A. Horne, T. Arpornthip, Z. Luo, A. J. Fallon, S. J. Berl, and C. A. Sackett, Quantum rotation sensing with dual Sagnac interferometers in an atom-optical waveguide, *Phys. Rev. Lett.* **124**, 120403 (2020).
- [156] R. Stevenson, M. R. Hush, T. Bishop, I. Lesanovsky, and T. Fernholz, Sagnac interferometry with a single atomic clock, *Phys. Rev. Lett.* **115**, 163001 (2015).
- [157] M. A. M. Marte and D. F. Walls, Enhanced sensitivity of fiber-optic rotation sensors with squeezed light, *J. Opt. Soc. Am. B* **4**, 1849 (1987).
- [158] M. Mehmet, T. Eberle, S. Steinlechner, H. Vahlbruch, and R. Schnabel, Demonstration of a quantum-enhanced fiber Sagnac interferometer, *Opt. Lett.* **35**, 1665 (2010).
- [159] X. Tian and K. Chen, The theoretical limit of sagnac effect, in *2018 Joint International Advanced Engineering and Technology Research Conference (JIAET 2018)* (Atlantis Press, 2018) pp. 435–441.
- [160] M. Fink, F. Steinlechner, J. Handsteiner, J. P. Dowling, T. Scheidl, and R. Ursin, Entanglement-enhanced optical gyroscope, *New J. Phys.* **21**, 053010 (2019).
- [161] M. R. Grace, C. N. Gagatsos, Q. Zhuang, and S. Guha, Quantum-enhanced fiber-optic gyroscopes using quadrature squeezing and continuous-variable entanglement, *Phys. Rev. Appl.* **14**, 034065 (2020).
- [162] K.-X. Sun, M. M. Fejer, E. Gustafson, and R. L. Byer, Sagnac interferometer for gravitational-wave detection, *Phys. Rev. Lett.* **76**, 3053 (1996).
- [163] B. Petrovichev, M. Gray, and D. McClelland, Simulating the performance of Michelson- and Sagnac-based laser interferometric gravitational wave detectors in the presence of mirror tilt and curvature errors, *Gen. Relativ. Gravit.* **30**, 1055 (1998).
- [164] J. Mizuno, A. Rüdiger, R. Schilling, W. Winkler, and K. Danzmann, Frequency response of Michelson- and Sagnac-based interferometers, *Opt. Commun.* **138**, 383 (1997).
- [165] S. H. Huttner, S. L. Danilishin, B. W. Barr, A. S. Bell, C. Gräf, J. S. Hennig, S. Hild, E. A. Houston, S. S. Leavey, D. Pascucci, B. Sorazu, A. P. Spencer, S. Steinlechner, J. L. Wright, T. Zhang, and K. A. Strain, Candidates for a possible third-generation gravitational wave detector: comparison of ring-Sagnac and sloshing-Sagnac speedmeter interferometers, *Class. Quantum Gravity* **34**, 024001 (2016).
- [166] N. V. Voronchev, S. L. Danilishin, and F. Y. Khalili, A Sagnac interferometer as a gravitational-wave third-generation detector, *Mosc. Univ. Phys. Bull.* **69**, 519 (2014).
- [167] S. H. Huttner, S. L. Danilishin, S. Hild, and K. A. Strain, Comparison of different sloshing speedmeters, *Class. Quantum Gravity* **37**, 085022 (2020).
- [168] P. Purdue, Analysis of a quantum nondemolition speedmeter interferometer, *Phys. Rev. D* **66**, 022001 (2002).
- [169] P. Purdue and Y. Chen, Practical speed meter designs for quantum nondemolition gravitational-wave interferometers, *Phys. Rev. D* **66**, 122004 (2002).
- [170] A. Freise, H. Miao, and D. D. Brown, Simplified optical configuration for a sloshing-speedmeter-enhanced gravitational wave detector, *Class. Quantum Gravity* **37**, 025007 (2019).
- [171] P. B. Dixon, D. J. Starling, A. N. Jordan, and J. C. Howell, Ultrasensitive beam deflection measurement via interferometric weak value amplification, *Phys. Rev. Lett.* **102**, 173601 (2009).
- [172] Y. Susa, Y. Shikano, and A. Hosoya, Optimal probe wave function of weak-value amplification, *Phys. Rev. A* **85**, 052110 (2012).
- [173] J. Dressel, K. Lyons, A. N. Jordan, T. M. Graham, and P. G. Kwiat, Strengthening weak-value amplification with recycled photons, *Phys. Rev. A* **88**, 023821 (2013).

- [174] A. N. Jordan, J. Martínez-Rincón, and J. C. Howell, Technical advantages for weak-value amplification: when less is more, *Phys. Rev. X* **4**, 011031 (2014).
- [175] S. Pang, J. Dressel, and T. A. Brun, Entanglement-assisted weak value amplification, *Phys. Rev. Lett.* **113**, 030401 (2014).
- [176] G. B. Alves, B. M. Escher, R. L. de Matos Filho, N. Zagury, and L. Davidovich, Weak-value amplification as an optimal metrological protocol, *Phys. Rev. A* **91**, 062107 (2015).
- [177] J. Harris, R. W. Boyd, and J. S. Lundeen, Weak value amplification can outperform conventional measurement in the presence of detector saturation, *Phys. Rev. Lett.* **118**, 070802 (2017).
- [178] Y. Aharonov, D. Z. Albert, and L. Vaidman, How the result of a measurement of a component of the spin of a spin-1/2 particle can turn out to be 100, *Phys. Rev. Lett.* **60**, 1351 (1988).
- [179] A. C. Elitzur and E. Cohen, The retrocausal nature of quantum measurement revealed by partial and weak measurements, in *AIP Conference Proceedings*, Vol. 1408 (American Institute of Physics, 2011) pp. 120–131.
- [180] E. Cohen and E. Pollak, Determination of weak values of quantum operators using only strong measurements, *Phys. Rev. A* **98**, 042112 (2018).
- [181] Y. Pan, J. Zhang, E. Cohen, C.-w. Wu, P.-X. Chen, and N. Davidson, Weak-to-strong transition of quantum measurement in a trapped-ion system, *Nat. Phys.* **16**, 1206 (2020).
- [182] J. Dziewior, L. Knips, D. Farfurnik, K. Senkalla, N. Benshalom, J. Efroni, J. Meinecke, S. Bar-Ad, H. Weinfurter, and L. Vaidman, Universality of local weak interactions and its application for interferometric alignment, *Proc. Natl. Acad. Sci.* **116**, 2881 (2019).
- [183] J. Martínez-Rincón, C. A. Mullarkey, G. I. Viza, W.-T. Liu, and J. C. Howell, Ultrasensitive inverse weak-value tilt meter, *Opt. Lett.* **42**, 2479 (2017).
- [184] E. Sjöqvist, Geometric phase in weak measurements, *Phys. Lett. A* **359**, 187 (2006).
- [185] Y.-W. Cho, Y. Kim, Y.-H. Choi, Y.-S. Kim, S.-W. Han, S.-Y. Lee, S. Moon, and Y.-H. Kim, Emergence of the geometric phase from quantum measurement back-action, *Nat. Phys.* **15**, 665 (2019).
- [186] V. Gebhart, K. Snizhko, T. Wellens, A. Buchleitner, A. Romito, and Y. Gefen, Topological transition in measurement-induced geometric phases, *Proc. Natl. Acad. Sci.* **117**, 5706 (2020).
- [187] Y. Wang, K. Snizhko, A. Romito, Y. Gefen, and K. Murch, Observing a topological transition in weak-measurement-induced geometric phases, [arXiv:2102.05660](https://arxiv.org/abs/2102.05660) (2021).
- [188] A. N. Jordan, P. Lewalle, J. Tollaksen, and J. C. Howell, Gravitational sensing with weak value based optical sensors, *Quantum Studies: Math. Found.* **6**, 169 (2019).
- [189] O. S. Magaña-Loaiza, M. Mirhosseini, B. Rodenburg, and R. W. Boyd, Amplification of angular rotations using weak measurements, *Phys. Rev. Lett.* **112**, 200401 (2014).
- [190] S.-Z. Fang, H.-T. Tan, G.-X. Li, and Q.-L. Wu, Weak value amplification for angular velocity measurements, *Appl. Opt.* **60**, 4335 (2021).
- [191] J.-H. Huang, X.-Y. Duan, and X.-Y. Hu, Amplification of rotation velocity using weak measurements in Sagnac's interferometer, *Eur. Phys. J. D* **75**, 114 (2021).
- [192] J. Larmor, *Aether and Matter* (University Press, 1900).
- [193] Y. Aharonov and G. Carmi, Quantum aspects of the equivalence principle, *Found. Phys.* **3**, 493 (1973).
- [194] J. H. Harris and M. D. Semon, A review of the Aharonov-Carmi thought experiment concerning the inertial and electromagnetic vector potentials, *Found. Phys.* **10**, 151 (1980).
- [195] J. Anandan, Curvature effects in interferometry, *Phys. Rev. D* **30**, 1615 (1984).
- [196] J. Anandan, Gravitational and rotational effects in quantum interference, *Phys. Rev. D* **15**, 1448 (1977).
- [197] J. Anandan, Interference, gravity and gauge fields, *Nuovo Cim. A* **53**, 221 (1979).
- [198] J. Anandan and B. Lesche, Interferometry in a space-time with torsion, *Lett. Nuovo Cim.* **37**, 391 (1983).
- [199] L. Ford and A. Vilenkin, A gravitational analogue of the Aharonov-Bohm effect, *J. Phys. A* **14**, 2353 (1981).
- [200] R. Y. Chiao, R. W. Haun, N. A. Inan, B.-S. Kang, L. A. Martinez, S. J. Minter, G. A. Munoz, and D. A. Singleton, A gravitational Aharonov-Bohm effect, and its connection to parametric oscillators and gravitational radiation, in *Quantum Theory: A Two-Time Success Story* (Springer, 2014) pp. 213–246.
- [201] V. Vedral, Geometric phases and topological quantum computation, *Int. J. Quantum Inf.* **1**, 1 (2003).
- [202] E. Sjöqvist, Geometric phases in quantum information, *Int. J. Quantum Chem.* **115**, 1311 (2015).
- [203] Z. Chen, Observable-geometric phases and quantum computation, *Int. J. Theor. Phys.* **59**, 1255 (2020).
- [204] A. Kuppermann and Y.-S. M. Wu, The geometric phase effect shows up in chemical reactions, *Chem. Phys. Lett.* **205**, 577 (1993).
- [205] B. K. Kendrick, J. Hazra, and N. Balakrishnan, The geometric phase controls ultracold chemistry, *Nat. Commun.* **6**, 7918 (2015).
- [206] Y. Aharonov, E. Cohen, F. Colombo, T. Landsberger, I. Sabadini, D. C. Struppa, and J. Tollaksen, Finally making sense of the double-slit experiment, *Proc. Natl. Acad. Sci.* **114**, 6480 (2017).
- [207] B. N. Bolotovskii and S. N. Stoliarov, Optical analog of the Magnus effect, *Pis'ma Zh. Eksp. Teor. Fiz.* **25**, 148 (1977).
- [208] B. Y. Zel'dovich and V. S. Liberman, Rotation of the plane of a meridional beam in a graded-index waveguide due to the circular nature of the polarization, *Soviet Journal of Quantum Electronics* **20**, 427 (1990).
- [209] A. V. Dooghin, N. D. Kundikova, V. S. Liberman, and B. Y. Zel'dovich, Optical Magnus effect, *Phys. Rev. A* **45**, 8204 (1992).
- [210] K. Y. Bliokh and Y. P. Bliokh, Topological spin transport of photons: the optical Magnus effect and Berry phase, *Physics Letters A* **333**, 181 (2004).
- [211] K. Y. Bliokh and Y. P. Bliokh, Modified geometrical optics of a smoothly inhomogeneous isotropic medium: the anisotropy, Berry phase, and the optical Magnus effect, *Phys. Rev. E* **70**, 026605 (2004).